Neuron, Vol. 35, 107–120, July 3, 2002, Copyright ©2002 by Cell Press

Ubiquitin and AP180 Regulate the Abundance of GLR-1 Glutamate Receptors at Postsynaptic Elements in *C. elegans*

Michelle Burbea,[2] Lars Dreier,[2] Jeremy S. Dittman, Maria E. Grunwald, and Joshua M. Kaplan[1,3]
Department of Molecular and Cell Biology
University of California
Berkeley, California 94720

Summary

Regulated delivery and removal of α-amino-3-hydroxy-5-methyl-4-isoxazolepropionic acid (AMPA) glutamate receptors (GluRs) from postsynaptic elements has been proposed as a mechanism for regulating synaptic strength. Here we test the role of ubiquitin in regulating synapses that contain a *C. elegans* GluR, GLR-1. GLR-1 receptors were ubiquitinated in vivo. Mutations that decreased ubiquitination of GLR-1 increased the abundance of GLR-1 at synapses and altered locomotion behavior in a manner that is consistent with increased synaptic strength. By contrast, overexpression of ubiquitin decreased the abundance of GLR-1 at synapses and decreased the density of GLR-1-containing synapses, and these effects were prevented by mutations in the *unc-11* gene, which encodes a clathrin adaptin protein (AP180). These results suggest that ubiquitination of GLR-1 receptors regulates synaptic strength and the formation or stability of GLR-1-containing synapses.

Introduction

Regulation of synaptic efficacy is thought to form the basis of information storage and processing in the brain. At central synapses, fast excitatory synaptic transmission is mediated primarily by two families of glutamate receptors (GluRs): α-amino-3-hydroxy-5-methyl-4-isoxazolepropionic acid (AMPA) receptors and *N*-methyl-D-aspartate (NMDA) receptors. Work from several laboratories suggests that regulation of the abundance of postsynaptic AMPA receptors is a potential mechanism for producing activity-dependent changes in synaptic strength. AMPA receptors present at postsynaptic elements are derived from a rapidly recycling pool of receptors undergoing repeated cycles of insertion by exocytosis and removal by endocytosis (Nishimune et al., 1998; Song et al., 1998; Luscher et al., 1999; Ehlers, 2000; Passafaro et al., 2001). Although the dynamic recycling of AMPA receptors is a relatively recent discovery, the biochemical mechanisms underlying this process are beginning to emerge. Treatments that block exocytosis diminish the levels of AMPA receptors found at postsynaptic elements (Luscher et al., 1999; Lu et al., 2001). AMPA receptors are removed from synaptic elements by clathrin-mediated endocytosis (Carroll et al., 1999a, 1999b; Luscher et al., 1999; Man et al., 2000). Endocytosis of AMPA receptors can be stimulated either by treatment with receptor agonists, receptor antagonists, or with insulin (Carroll et al., 1999a; Beattie et al., 2000; Ehlers, 2000; Lin et al., 2000; Man et al., 2000; Liang and Huganir, 2001; Snyder et al., 2001).

The dynamic process of AMPA receptor insertion and removal from the postsynaptic membrane is required for induction of long-term potentiation (Lledo et al., 1998) and long-term depression (Luscher et al., 1999; Luthi et al., 1999; Man et al., 2000; Wang and Linden, 2000). These results suggest that the cell biological mechanisms governing AMPA receptor exo- and endocytosis play a pivotal role in producing activity-dependent changes in synaptic strength; however, much remains to be learned about the detailed mechanisms controlling AMPA receptor abundance at synapses.

Covalent modification of proteins with ubiquitin has been shown to target proteins for degradation by the proteasome, and to regulate intracellular trafficking of some membrane proteins (Hochstrasser, 1996; Hicke, 1999; Helliwell et al., 2001; Katzmann et al., 2001; Reggiori and Pelham, 2001; Urbanowski and Piper, 2001). Ubiquitin-mediated regulation of protein stability has been shown to play a role in several processes, including synaptic plasticity. For example, long-term facilitation of synaptic strength in *Aplysia* is dependent upon proteasomal degradation of the regulatory subunit of the cyclic AMP-dependent protein kinase (Hegde et al., 1997; Chain et al., 1999). Ubiquitination has also been implicated in hippocampal long-term potentiation in mice (Jiang et al., 1998) and in growth of presynaptic nerve terminals in *Drosophila* (DiAntonio et al., 2001); however, in these cases, the substrates involved have not been identified. Taken together, these results suggested that ubiquitination of synaptic proteins may contribute to the regulation of synapse structure and function.

We have utilized the nematode *C. elegans* as a simple model to study the mechanisms by which AMPA receptors are regulated. The *C. elegans* genome encodes eight non-NMDA ionotropic receptor subunits (Brockie et al., 2001), one of which is encoded by the *glr-1* gene (Hart et al., 1995; Maricq et al., 1995). Mutants lacking the *glr-1* GluR are defective for a specific mechanosensory behavior, avoidance of nose touch (Hart et al., 1995; Maricq et al., 1995). The *glr-1* GluRs are expressed in ventral cord interneurons (Hart et al., 1995; Maricq et al., 1995), where they are localized at sensory-interneuron synapses (Rongo et al., 1998). Trafficking of *glr-1* GluRs from interneuron cell bodies to the ventral nerve cord is regulated by CaMKII and voltage-gated calcium channels, suggesting that activity-dependent mechanisms regulate GLR-1 receptor trafficking in *C. elegans* (Rongo and Kaplan, 1999). However, since in this case activity has been altered chronically, that is by mutations, these changes in GLR-1 trafficking may be caused by homeostatic compensatory mechanisms rather than by acute changes in activity. Here we show that *glr-1* GluR abun-

[1]Correspondence: joshkap@socrates.berkeley.edu
[2]These authors contributed equally to this work.
[3]Present address: Department of Molecular Biology, Wellman 8, Massachusetts General Hospital, Boston, Massachusetts 02114.

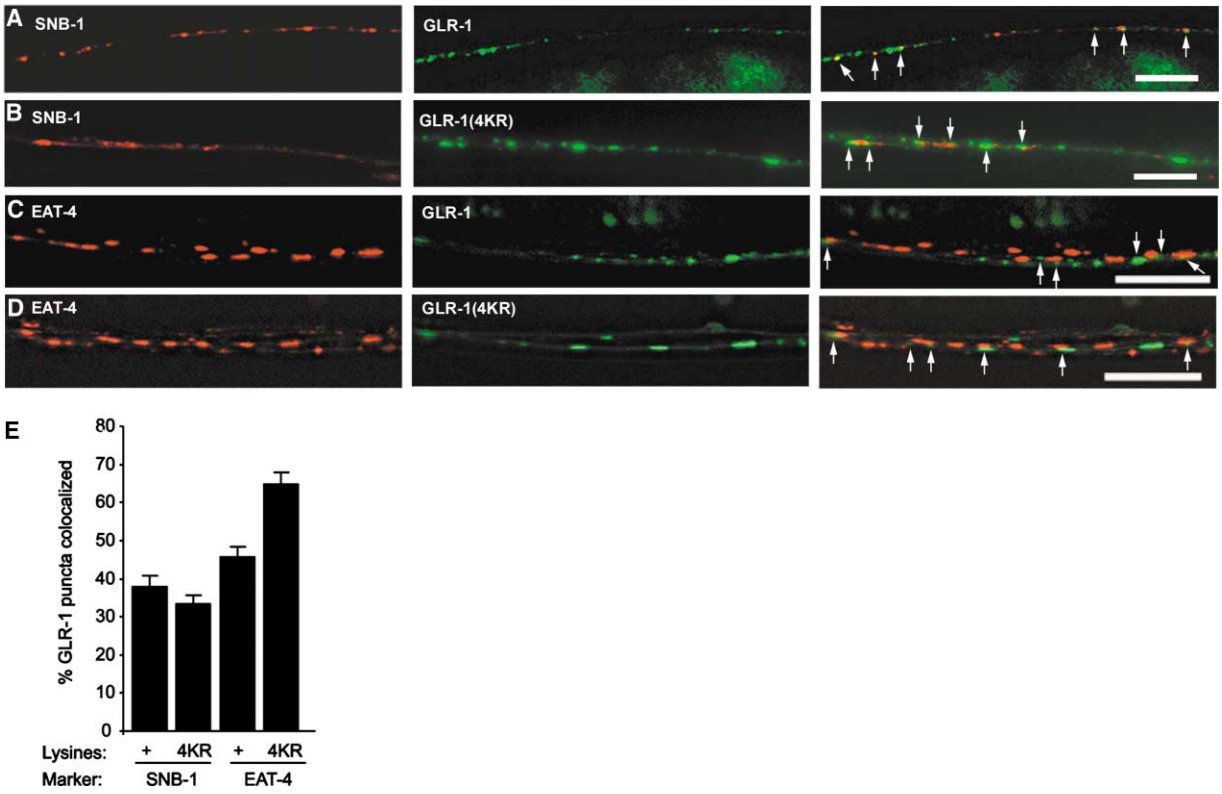

Figure 1. GLR-1 and GLR-1(4KR) Were Localized to Postsynaptic Elements

Localization of CFP-tagged synaptobrevin (SNB-1, A and B) expressed in ventral cord interneurons (using the *glr-1* promoter), and of YFP-tagged *eat-4* VGLUT expressed with the *eat-4* promoter (C and D), are shown in red in the left hand panels. Localization of YFP-tagged (A and B) and CFP-tagged (C and D) wild-type GLR-1 (A and C) or GLR-1(4KR) (B and D) expressed in ventral cord interneurons is shown in green in the middle panels. Colocalization (arrows) of SNB-1 or EAT-4 with GLR-1 is shown in the merged images (right hand panels). (A and B) GLR-1 (A) and GLR-1(4KR) (B) puncta were closely apposed to SNB-1 puncta at interneuron-interneuron synapses. (C and D) GLR-1 (C) and GLR-1(4KR) (D) puncta were closely apposed to EAT-4 puncta at glutamatergic synapses. (E) The fraction of GLR-1 puncta that colocalized with SNB-1 and EAT-4 was determined as described in the Experimental Procedures. Scale bars are 10 μm.

dance at postsynaptic elements is regulated by clathrin-mediated endocytosis and by ubiquitination.

Results

GLR-1::GFP Is Properly Localized to Postsynaptic Elements

We previously showed that a GFP-tagged version of the *glr-1* GluR (GLR-1::GFP) could be used to visualize synaptic elements in transgenic worms (Figure 1A) (Rongo et al., 1998; Rongo and Kaplan, 1999). Transgene-encoded GLR-1::GFP receptors were expressed in ventral cord interneurons (which express the endogenous *glr-1* GluRs), and were found in punctate structures in the ventral nerve cord. These ventral cord puncta colocalize with synaptobrevin at sensory-interneuron synapses (Rongo et al., 1998). To further document the synaptic targeting of GLR-1::GFP, we analyzed GLR-1 localization with two presynaptic markers: synaptobrevin (SNB-1, Figure 1A) and the vesicular glutamate transporter (VGLUT, Figure 1C), which is encoded by the *eat-4* gene (Lee et al., 1999; Bellochio et al., 2000; Takamori et al., 2000). In principle, the best test of GLR-1 colocalization with presynaptic markers would be to label all nerve termini, e.g., by staining with anti-synaptobrevin antibodies; however, this experiment is not practical because the synaptic density in the ventral cord is so high that individual synapses cannot be resolved. Therefore, we restricted expression of the presynaptic markers to a subpopulation of nerve terminals. The SNB-1 fluorescent protein was expressed in the *glr-1*-expressing interneurons, labeling interneuron-interneuron synapses. The *eat-4* VGLUT fluorescent protein was used to label a distinct set of synapses, since the *eat-4* promoter driving expression of this construct is not expressed in the *glr-1*-expressing interneurons (Lee et al., 1999) (M.G. and J.K., unpublished data). We found that GLR-1::GFP puncta were often closely apposed to both SNB-1 (38% ± 3%) and EAT-4 (46% ± 3%) puncta (Figure 1E). Since the SNB-1 and EAT-4 markers label nonoverlapping sets of synapses, these results suggest that a large fraction of the GLR-1::GFP puncta (>80%) correspond to postsynaptic elements.

The incomplete colocalization of GLR-1 with presynaptic markers is predicted for two reasons. First, failure of GLR-1 to completely colocalize with EAT-4 was expected because additional VGLUT encoding genes are predicted by the *C. elegans* genome sequence. Second, the GLR-1-expressing interneurons have multiple synaptic inputs, of which only a subset expresses the *eat-4*

VGLUT and SNB-1 transgenes (White et al., 1986; Lee et al., 1999). In the case of interneuron-interneuron synapses, we were able to estimate the extent of colocalization from the known connectivity. The GLR-1-expressing interneurons have a total of 451 synaptic inputs in the ventral nerve cord, of which 120 (27%) are interneuron-interneuron synapses (White et al., 1986). It is not surprising that the fraction colocalized observed in our experiment (38% ± 3%, Figure 1E) was somewhat higher than that predicted since GLR-1 receptors are not present at all postsynaptic elements in these interneurons (M.G. and J.K., unpublished data), and because we analyzed a specific region of the ventral nerve cord.

The *unc-11* AP180 Clathrin Adaptin Protein Controls the Abundance of GLR-1::GFP at Synapses

The numbers and sizes of these *glr-1* GluR containing puncta in the ventral cord can be measured by quantitative fluorescence microscopy. To estimate the total abundance of GLR-1::GFP at ventral cord puncta, we measured the peak amplitude of fluorescence in each punctum, and the width of each punctum. Puncta amplitudes were measured as the fractional increase in GLR-1::GFP fluorescence in puncta over the diffuse background of fluorescence in the ventral cord (%ΔF/F). We measured the density of GLR-1::GFP puncta in the ventral cord to estimate the density of GLR-1-containing synapses. Since GFP was inserted into a cytoplasmic domain of GLR-1, GLR-1::GFP molecules in the plasma membrane and in subsynaptic endosomal compartments should contribute equally to the total fluorescence of each punctum. Therefore, the fluorescence measurements reported here likely correspond to the sum of plasma membrane and endosomal receptor pools and recycling of receptors between the endosome and plasma membrane should not contribute to changes in fluorescence. We used quantitative fluorescence microscopy to examine the mechanisms regulating the abundance and distribution of GLR-1::GFP in the ventral nerve cord.

Recent results from several labs suggest that mammalian AMPA receptors are removed from postsynaptic membranes by clathrin-mediated endocytosis (Carroll et al., 1999a, 1999b; Luscher et al., 1999; Man et al., 2000). Consistent with these results, we isolated *nu428*, a mutation in the *unc-11* gene, in a screen for mutants that have increased abundance of GLR-1::GFP in the ventral nerve cord (data not shown). Similar defects in GLR-1::GFP abundance were observed in other *unc-11* mutants, including strains carrying the putative null allele, *e47* (Figure 2). The *unc-11* gene encodes a clathrin adaptin protein AP180 (Nonet et al., 1999). AP180 is a soluble adaptor protein that has been implicated in recruiting clathrin to endocytic cargo proteins (Kirchhausen, 1999). In both *Drosophila* and *C. elegans*, mutants lacking AP180 have endocytic defects (Zhang et al., 1998; Nonet et al., 1999).

Two principal defects were observed in the distribution of GLR-1::GFP in *unc-11* AP180 mutants. First, in the anterior most region of the ventral nerve cord, we observed highly abundant and diffusely distributed GLR-1::GFP in *unc-11* AP180 mutants whereas wild-type animals retained modestly sized puncta in the same region (Figures 2A and 2B). In more posterior regions of the ventral nerve cords of *unc-11* AP180 mutants, GLR-1::GFP remained punctate, but the puncta were significantly larger and brighter than those observed in wild-type animals (Figures 2D, 2E, and 2G). Both of these defects in receptor distribution were corrected by vectors driving expression of wild-type *unc-11* AP180 cDNA constructs with the *glr-1* promoter (Figures 2C, 2F, and 2G), indicating that both defects were caused by the absence of *unc-11* AP180 from GLR-1-expressing neurons.

Changes in puncta sizes and puncta densities were measured by quantitative fluorescence microscopy (Figures 2G and 2H). These analyses showed that mean puncta amplitude and width were both significantly increased in *unc-11* AP180 mutants as compared to wild-type controls. By contrast, puncta densities observed in *unc-11* AP180 mutants were indistinguishable from those found in wild-type animals. These results suggest that AP180 and, by inference, clathrin-mediated endocytosis regulate the abundance of *glr-1* GluRs in the ventral cord. In addition, as deficient endocytosis was associated with increased GLR-1::GFP fluorescence, our results also suggest that a significant fraction of endocytosed GLR-1 receptors is degraded.

The change in the average dimensions of *unc-11* AP180 mutant puncta could reflect a global change in all ventral cord puncta. Alternatively, a select subpopulation of ventral cord puncta could be particularly sensitive to steady-state changes in the rate of endocytosis. To distinguish between these possibilities, we compared the distributions of puncta amplitudes and widths in *unc-11* AP180 versus wild-type ventral nerve cords (Figure 2H). We found that the wild-type puncta amplitude distribution was well fit by a scaled version of the *unc-11* AP180 distributions. In the case of puncta widths, the *unc-11* AP180 mutation had a slightly disproportionate effect on larger puncta. These results suggest that *unc-11* AP180 globally regulates the abundance of GLR-1 receptors across the entire population of ventral cord puncta.

Overexpression of Ubiquitin Decreases GLR-1::GFP Puncta Amplitude and Puncta Density

The concentration of monoubiquitin has been shown to be rate limiting for ubiquitination (Papa and Hochstrasser, 1993; Hegde et al., 1997; Swaminathan et al., 1999). Therefore, we reasoned that overexpression of ubiquitin might promote increased ubiquitination of target proteins. To determinine if ubiquitin regulates the distribution of GLR-1::GFP in the ventral cord, we constructed a transgene which expresses ubiquitin tagged with nine copies of the Myc epitope (MUb) in these ventral cord interneurons. We found that the MUb transgene (*nuIs89*) greatly reduced density and amplitudes of GLR-1::GFP-containing puncta, whereas puncta widths were not significantly altered (Figure 3). Therefore, these results are consistent with the idea that ubiquitin directly or indirectly induces degradation of *glr-1* GluRs.

Since puncta amplitudes and puncta density were both significantly diminished upon overexpression of MUb (Figure 3D), it was possible that the change in puncta density was a secondary consequence of the

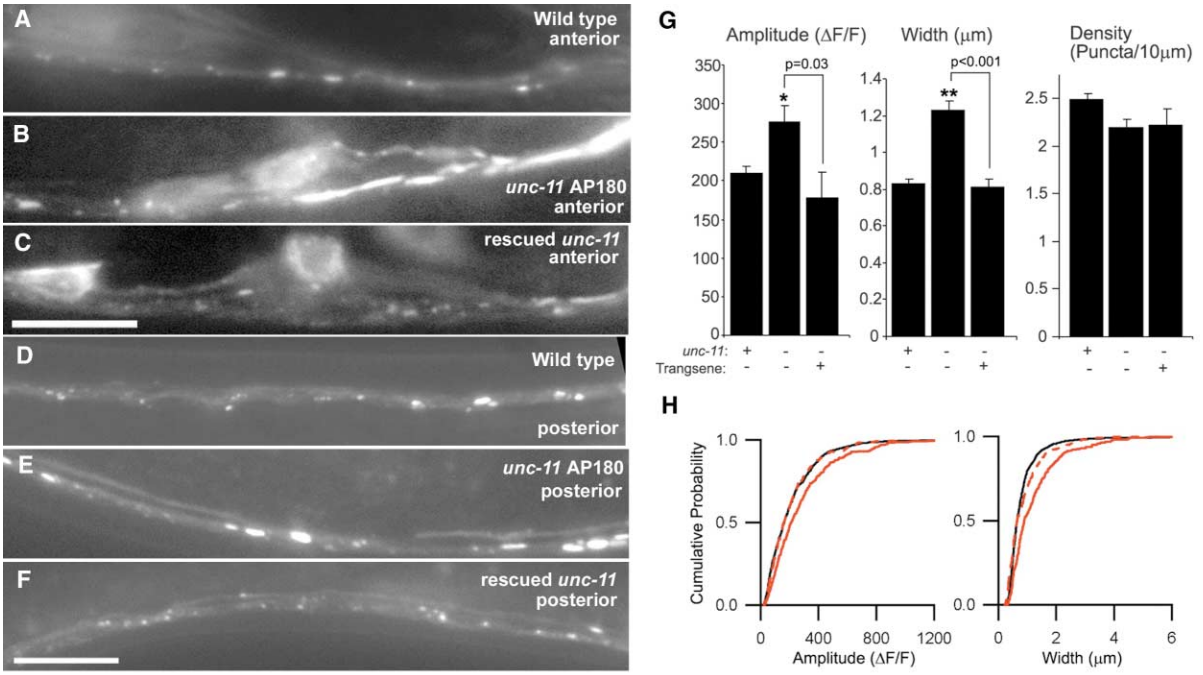

Figure 2. Mutants Lacking *unc-11* AP180 Had Increased Abundance of GLR-1::GFP in the Ventral Nerve Cord

Representative images of GLR-1::GFP (*nuIs24*) in the ventral nerve cords of wild-type (A and D), *unc-11(e47)* AP180 (B and E), and transgenic *unc-11(e47)* AP180 mutant animals carrying a transgene that expresses wild-type *unc-11* AP180 cDNAs in the GLR-1-expressing interneurons (C and F) are shown. In an anterior region of the ventral cord (A–C), between the nerve ring and the RIG neuron cell bodies, GLR-1::GFP accumulated in bright diffuse patches of fluorescence in *unc-11(e47)* AP180 mutants (B), whereas a punctate pattern was observed in wild-type (A) and in *unc-11(e47)* AP180 mutants rescued with the *unc-11(+)* transgene (C). In a more posterior region of the nerve cord (D–F), between the RIG cell bodies and the vulva, puncta widths and amplitudes were significantly increased in *unc-11(e47)* AP180 mutants (E) compared to wild-type (D) or to *unc-11(e47)* AP180 mutants rescued with the *unc-11(+)* transgene (F). A 10 μm scale bar for (A)–(C) is shown in (C), and for (D)–(F) in (F). Puncta amplitudes, widths, and densities in the more posterior region are compared in wild-type, *unc-11(e47)* AP180, and rescued *unc-11(e47)* AP180 mutants (G). Values that differ significantly from wild-type controls are indicated as follows: *, $p < 0.01$; and **, $p < 0.001$. (H) Amplitude and width distributions of wild-type (black) and *unc-11(e47)* mutant (red) puncta are compared. The amplitudes and widths of *unc-11(e47)* mutant puncta are uniformly shifted to larger values than those observed in wild-type. A 29% reduction in the *unc-11(e47)* amplitude and a 38% reduction in the width distributions are shown as the dashed red lines.

change in receptor abundance at each punctum. Specifically, we would expect that a certain fraction of ventral cord puncta would no longer be detectable above the diffuse background of ventral cord fluorescence after expression of MUb. We estimated that following a 54% decrease in amplitude, 15% of wild-type puncta would be lost as their amplitudes would be less than the smallest detected MUb punctum. By contrast, we observed an 82% decline in puncta density in strains expressing MUb (Figure 3D). As a second independent method to measure the relationship between puncta density and receptor abundance, we compared the density of ventral cord puncta in two transgenic strains expressing different levels of wild-type GLR-1::GFP (*nuIs24* and *nuIs25*). From quantitative Western blots, we estimated that the GLR-1::GFP abundance in *nuIs25* was 52% that found in *nuIs24* (Table 1). We found that *nuIs24* puncta amplitudes were significantly greater than those observed in *nuIs25* animals, whereas puncta widths and densities were indistinguishable in these strains (Figure 4). Interestingly, the difference in puncta amplitudes between *nuIs24* and *nuIs25* (42%) was similar to the amplitude reduction caused by MUb (54%), yet the two wild-type strains had identical widths and densities. Therefore, changes in puncta amplitudes are unlikely to explain the MUb-induced decrease in puncta densities. We conclude that overexpression of ubiquitin independently regulates both the abundance of GLR-1 at each punctum and the number of GLR-1-containing puncta.

glr-1 GluRs Are Ubiquitinated In Vivo

MUb-induced decrease in puncta amplitudes and densities could result from direct ubiquitination of *glr-1* GluRs or ubiquitination of other, unidentified proteins. We tested whether *glr-1* GluRs are ubiquitinated through a variety of experiments. First, we tested whether MUb was conjugated to GLR-1::GFP in transgenic animals (Figure 5A). We detected the GLR-1::GFP fusion protein with anti-GFP in immunoblots or immunoprecipitations using a membrane fraction isolated from worm extracts. Immunoblotting with anti-Myc identified one major and several minor MUb-GLR-1 bands in immunoprecipitates formed with anti-GFP.

It is possible that the MUb-GLR-1 conjugates observed were a consequence of overexpression of MUb. To control for this possibility, we tested whether GLR-1::GFP formed conjugates with endogenously expressed ubiquitin (Figure 5B). In this case, Ub-GLR-1 conjugates were detected by performing a double immunoprecipitation protocol, using anti-GFP and anti-

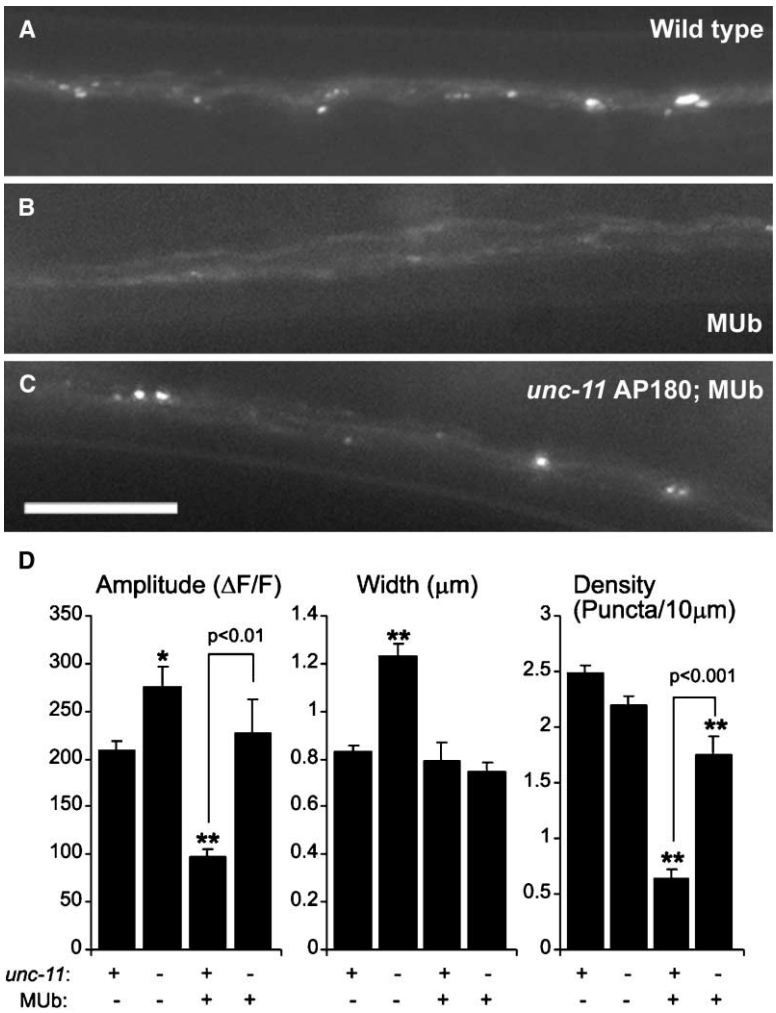

Figure 3. Expression of the MUb Transgene Decreased GLR-1::GFP Puncta Amplitudes and Puncta Density

The distribution of GLR-1::GFP in the ventral nerve cords of wild type (A), *nuIs89* MUb (B), and *unc-11(e47)*; *nuIs89* MUb double mutants (C) are compared. Average puncta amplitudes, widths, and densities are shown in (D). *nuIs89* MUb animals had a lower density of puncta, and each punctum had a lower fluorescence intensity than in wild-type controls. The ubiquitin-induced decrease in puncta fluorescence was prevented by the *unc-11(e47)* AP180 mutation. The *unc-11(e47)* AP180 mutation also significantly reduced the effect of ubiquitin on puncta density. Values that differ significantly from wild-type controls are indicated as follows: * indicates $p < 0.01$; and ** indicates $p < 0.001$. A 10 μm scale bar is shown in (C).

ubiquitin, followed by immunoblotting with anti-GFP. Here again we were able to detect Ub-GLR-1 conjugates as a doublet of higher molecular weight species. These higher molecular weight species were not detected when normal rabbit serum was used in the second immunoprecipitation (data not shown), nor when anti-ubiquitin was saturated with purified ubiquitin prior to the second immunoprecipitation. We were also able to detect Ub-GLR-1 conjugates by immunoblotting with anti-ubiquitin antibodies following immunoprecipitation with

Table 1. Comparison of the Transgenics Strains Analyzed

Genotype	GFP Abundance[a]	Normalized GFP Abundance[b]	Line Scans	Puncta
nuIs24 GLR-1::GFP	5.0 ± 0.5	1.0	76	1461
nuIs25 GLR-1::GFP	2.6 ± 0.2	0.52	20	421
nuIs108 GLR-1(4KR)::GFP	3.4 ± 0.4	0.68	18	452
nuIs88 GLR-1(K888R)::GFP	4.0 ± 0.5	0.80	67	1367
unc-11(e47) AP180; *nuIs24* GLR-1::GFP	5.0 ± 0.4	1.0	19	377
unc-11(e47) AP180; *nuIs24* GLR-1::GFP; *unc-11(+)* transgene	ND	ND	7	128
unc-11 (e47); nuIs108 GLR-1(4KR)::GFP	ND	ND	33	712
nuIs89 MUb; *nuIs24* GLR-1::GFP	0.7 ± 0.1	0.14	21	76
nuIs89 MUb; *nuIs108* GLR-1(4KR)::GFP	ND	ND	18	149
unc-11(e47) AP180; *nuIs89* MUb; *nuIs24*	ND	ND	18	236

The number of line scans of ventral cord fluorescence, and the number of GLR-1::GFP puncta analyzed for each genotype are shown.
[a] Expression levels of GLR-1::GFP in some transgenic strains were compared by quantitative Western blots with anti-GFP. GFP abundance in these strains is reported as mean ± standard error of chemiluminescence (arbitrary units)/μg of total protein (N = 6–12 for each data point).
[b] Normalized differences in GFP abundance were also reported, where the levels found in *nuIs24* GLR-1::GFP were set as 1.0. ND indicates that this value has not been determined.

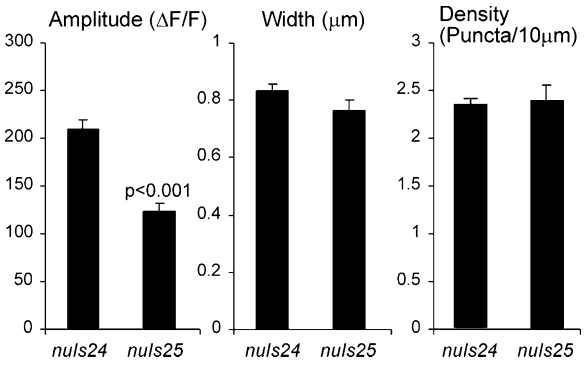

Figure 4. Effects of Transgene Expression Levels on GLR-1::GFP Puncta Amplitudes and Widths

The average puncta amplitudes, widths, and density are compared in two strains that express different levels of wild-type GLR-1::GFP, *nuls24*, and *nuls25*. In *nuls25* animals, GLR-1::GFP was expressed at 52% the levels found in *nuls24* animals, as determined by quantitative Western blots (Table 1). Values that differ significantly are indicated by their p values (Student's t test).

anti-GFP antibodies (Figure 5C). Thus, the presence of Ub-GLR-1 conjugates could not be ascribed to overexpression of MUb. From their mobility in gels, we estimated that the major MUb-GLR-1 and Ub-GLR-1 conjugates had fewer than five copies of the ubiquitin moiety. The MUb-GLR-1 species migrated more slowly than the Ub-GLR-1 conjugates, as would be predicted since the MUb protein contains nine copies of the Myc epitope. We estimated that the Ub-GLR-1 species represented less than 1% of the total GLR-1::GFP. It was not surprising that such a small fraction of receptors are found as Ub-GLR-1 conjugates since no effort was taken to prevent degradation of these conjugates. We were unable to detect conjugates formed between endogenously expressed *glr-1* GluRs and ubiquitin (data not shown); however, we would not expect to detect these endogenous Ub-GLR-1 conjugates since our anti-GLR-1 was not sufficiently sensitive to detect the minor fraction of endogenously expressed GLR-1 receptors that would be predicted to carry the ubiquitin tag. We conclude that *glr-1* GluRs are ubiquitinated but that these conjugates do not form extensive polyubiquitin chains.

Our analysis suggested that the major species of Ub-GLR-1 conjugates contained fewer than five ubiquitin or MUb moieties (Figure 5). Efficient degradation of ubiquitin conjugates by the proteasome requires the presence of polyubiquitin chains containing at least four ubiquitin moieties (Thrower et al., 2000); therefore, it remained possible that Ub-GLR-1 were degraded by the proteasome. It was also possible that more extensive polyubiquitin chains were assembled on GLR-1 but that these were not detected due to their rapid degradation. To further address whether ubiquitin regulation of *glr-1* GluR abundance is dependent on mono- or polyubiquitination, we expressed a mutant form of ubiquitin (K48R), which has a reduced ability to form polyubiquitin chains. Expression of MUb(K48R) transgenes, like wild-type MUb, significantly reduced the abundance of GLR-1::GFP in the ventral nerve cord (data not shown). This result suggests that degradation of GLR-1 does not require formation of extensive polyubiquitin chains.

Mutations that Prevent Formation of Ub-GLR-1 Conjugates Caused Increased Accumulation of GLR-1::GFP in the Ventral Nerve Cord

Ubiquitin moieties are conjugated to target proteins by forming isopeptide bonds with lysine residues in the

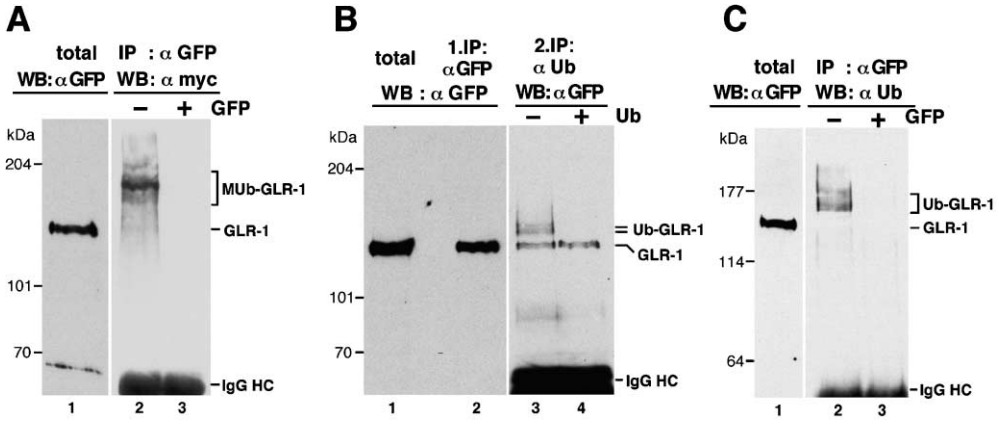

Figure 5. GLR-1::GFP Was Ubiquitinated In Vivo

(A) MUb-GLR-1 conjugates were detected in animals carrying both the *nuls24* GLR-1::GFP and the *nuls89* MUb transgenes. Total GLR-1::GFP in a membrane fraction was detected by immunoblotting with anti-GFP (lane 1). Immunoprecipitates formed with membrane extracts (50× that used in lane 1) and anti-GFP (lane 2) or with anti-GFP that had been saturated with purified GFP (lane 3) were immunoblotted with anti-Myc. (B) Ub-GLR-1 conjugates formed between GLR-1::GFP and endogenously expressed ubiquitin were detected in a double immunoprecipitation protocol. Total GLR-1::GFP in membranes isolated from *nuls24* GLR-1::GFP animals was detected by immunoblotting with anti-GFP (lane 1). Immunoprecipitates formed with *nuls24* GLR-1::GFP membranes and anti-GFP (lanes 2–4) were either directly immunoblotted with anti-GFP (lane 2), or were subjected to a second immunoprecipitation with anti-ubiquitin (lane 3) or with anti-ubiquitin that had first been saturated with purified ubiquitin (lane 4). For lanes 3 and 4, the amount of membranes was 100× that used in lanes 1 and 2. Note that a variable amount of unconjugated GLR-1::GFP contaminated the second immunoprecipitation (lanes 3 and 4). (C) Ub-GLR-1 conjugates were also detected by immunoblotting with anti-ubiquitin. Immunoprecipitates formed with anti-GFP (lane 2) or with anti-GFP that had been first saturated with purified GFP (lane 3) were immunoblotted with either anti-GFP (lane 1) or with anti-ubiquitin (lanes 2 and 3).

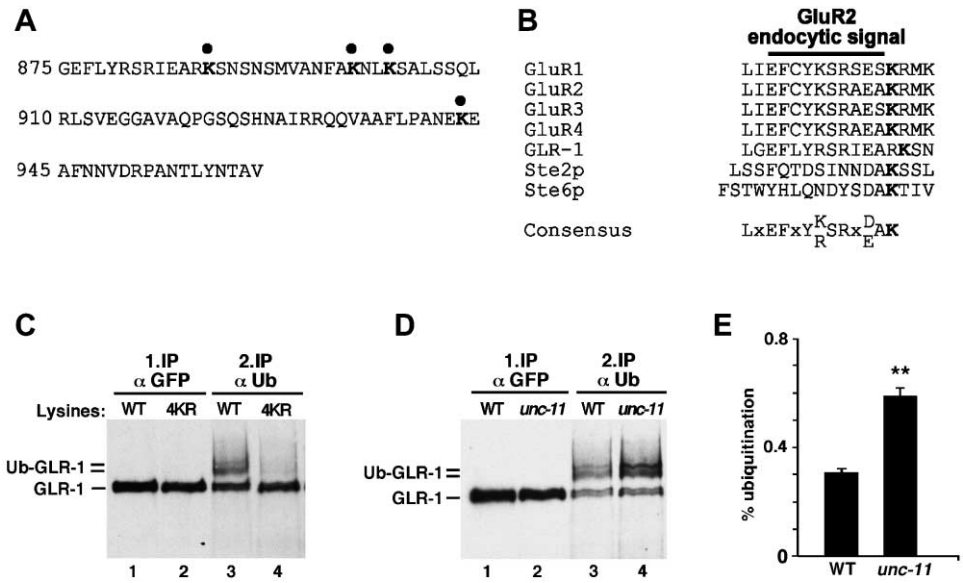

Figure 6. Role of GLR-1 Cytoplasmic Lysine Residues and AP180 in Forming Ub-GLR-1 Conjugates

(A) The sequence of the cytoplasmic tail of GLR-1 contains four lysine residues (black dots). (B) The sequence motif surrounding K888 is conserved in all mammalian AMPA receptors and bears some similarity to the ubiquitin/endocytosis signal in the yeast Ste2p and Ste6p proteins. Residues of GluR2 previously implicated in AMPA-induced endocytosis of GluR2 are indicated by the closed bar (Lin et al., 2000). (C) Mutant receptors lacking all four cytoplasmic lysine residues, GLR-1(4KR)::GFP, formed significantly fewer Ub-GLR-1 conjugates. Membrane extracts prepared from either *nuIs24* GLR-1::GFP (lanes 1 and 3) or *nuIs108* GLR-1(4KR)::GFP (lanes 2 and 4) were used for double immunoprecipitations, as in Figure 5. (D) Ub-GLR-1 conjugates were more abundant in *unc-11(e47)* AP180 mutants than in wild-type controls. GLR-1 receptors were immunoprecipitated from either *nuIs24* GLR-1::GFP (lanes 1 and 3) or *unc-11* AP180; *nuIs24* GLR-1::GFP (lanes 2 and 4) as in panel C. (E) Results from (D) were quantified from ten experiments. WT refers to *nuIs24* GLR-1::GFP and *unc-11* refers to *unc-11(e47)*; *nuIs24* GLR-1::GFP. ** Indicates that this value differs significantly ($p < 0.001$) from the wild-type control.

target protein. The cytosolic domains of *glr-1* GluRs contain four lysine residues (Figure 6A), of which K888 falls in a sequence that is conserved in the mammalian AMPA receptors (Figure 6B). This sequence motif shares some similarity with endocytic signals found in Ste2p and Ste6p, two yeast proteins which undergo ubiquitin-dependent endocytosis. We tested the importance of this motif by changing K888 to arginine. The average GLR-1(K888R) puncta amplitudes and widths were significantly greater than those observed in wild-type controls (Figures 7B, 7G, and 7H); however, average puncta densities were not significantly different from those observed with wild-type GLR-1::GFP (Figure 7I). Mutation of all four cytoplasmic lysine residues to arginine, GLR-1(4KR), caused an increase in puncta widths and a slight (albeit significant) increase in puncta densities compared to wild-type animals (Figures 7C, 7G–7I). GLR-1(4KR) puncta amplitudes were not significantly different from wild-type amplitudes. Since total receptor at each synapse is a function of both puncta amplitude and width, these results indicate that increased levels of GLR-1(K888R) and GLR-1(4KR) were found at postsynaptic elements as compared to wild-type controls. In both cases, the K888R and 4KR mutations uniformly increased puncta fluorescence across the entire distribution of ventral cord puncta (Figure 7K, and data not shown).

A possible explanation for these results was that changes in puncta amplitudes and widths observed in lysine mutants were caused by differences in the expression of the wild-type and mutant GLR-1::GFP transgenes. We controlled for this possibility in three ways. First, we showed that *nuIs88* GLR-1(K888R)::GFP and *nuIs108* GLR-1(4KR)::GFP animals expressed less total GLR-1::GFP than did the control strain (*nuIs24*) expressing wild-type receptors, by quantitative Western blots (Table 1). Thus, the increased puncta fluorescence observed in the lysine mutants could not be ascribed to increased total GLR-1::GFP abundance. Second, we compared puncta amplitudes, widths, and densities in animals expressing different levels of wild-type GLR-1::GFP (*nuIs24* and *nuIs25*) (Table 1). We found that differences in transgene expression could explain changes in puncta amplitudes but that differences in expression would not be expected to cause changes in puncta widths or densities (Figure 4). Third, we examined the distribution of GLR-1 in strains carrying a low copy transgene, which expressed GLR-1(4KR)::GFP at 56% the level found in *nuIs108* animals (as measured by ventral cord fluorescence), and found that puncta widths were significantly wider (1.17 ± 0.07 μm) than those found in animals expressing wild-type receptors (0.83 ± 0.02 μm). Taken together, these results suggested that the increased abundance of GLR-1(K888R) and GLR-1(4KR) receptors at postsynaptic elements could not be ascribed to differences in transgene expression levels.

The increased accumulation of GLR-1(4KR)::GFP at ventral cord puncta may have resulted from targeting of receptors to nonsynaptic sites. We did two experiments to test this possibility. First, we tested whether GLR-1(4KR)::YFP receptors were colocalized with sy-

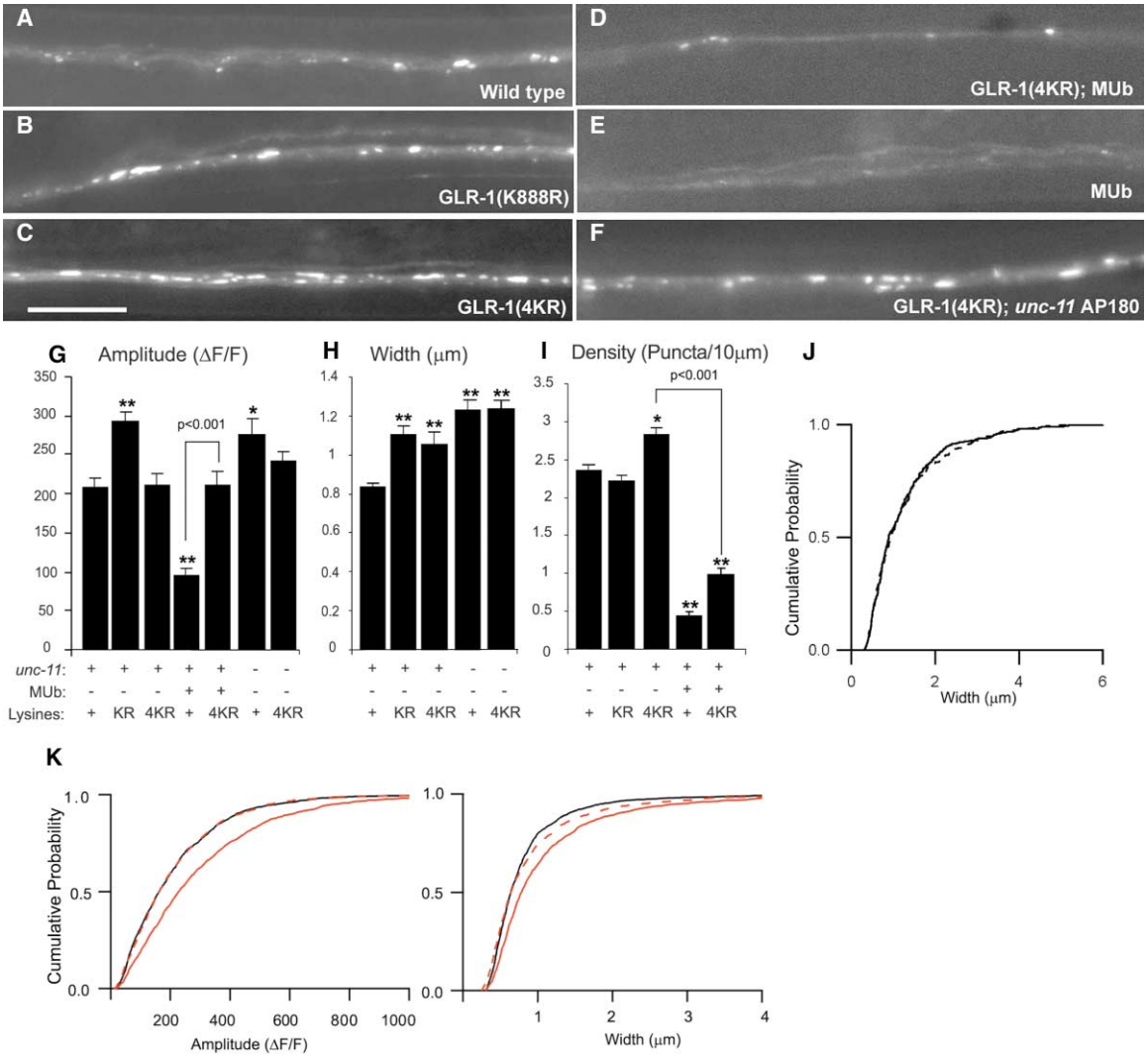

Figure 7. Lysine Mutations Alter GLR-1::GFP Puncta Amplitudes and Widths

Representative images of ventral cord fluorescence are shown for *nuIs24* GLR-1::GFP (A), *nuIs88* GLR-1(K888R)::GFP (B), *nuIs108* GLR-1(4KR)::GFP (C), *nuIs108* GLR-1(4KR)::GFP; *nuIs89* MUb double mutants (D), *nuIs24* GLR-1::GFP; *nuIs89* MUb (E), and *unc-11(e47)* AP180; *nuIs108* GLR-1(4KR)::GFP double mutants (F). Scale bar indicates 10 μm. The average puncta amplitudes (G), widths (H), and density (I) for the genotypes shown in (A)–(F) are compared. Values that differ significantly from wild-type controls are indicated as follows: * indicates $p < 0.01$; and ** indicates $p < 0.001$. (J) The puncta width distributions of *unc-11(e47)* AP180 (solid line) and *unc-11(e47)* AP180; *nuIs108* GLR-1(4KR)::GFP double mutants (dashed line) are indistinguishable, suggesting that the defects observed in these two mutants were not additive. (K) Amplitude and width distributions of wild-type (black) and *nuIs88* GLR-1(K888R)::GFP (red) puncta are compared. The amplitudes and widths of K888R puncta were shifted to smaller values than those observed in wild-type. A 40% reduction in the K888R amplitude and a 20% reduction in K888R width distributions are shown as the dashed red lines.

naptobrevin and *eat-4* VGLUT (Figures 1B, 1D, and 1E). We found that GLR-1(4KR) puncta were often closely apposed to SNB-1 puncta (33% ± 4%) and to EAT-4 puncta (65% ± 3%) (Figure 1E). Second, we showed that GLR-1(4KR)::GFP mutant receptors could functionally replace endogenously expressed GLR-1 receptors, which are required for responsiveness to nose touch stimuli. We found that *nuIs108* GLR-1(4KR)::GFP; *glr-1(n2461)* GluR double mutants were significantly more responsive to nose touch than were *glr-1(n2461)* GluR single mutants (93% ± 3% versus 4% ± 2% positive responses). Therefore, GLR-1(4KR)::GFP mutant receptors were both functionally competent, and correctly targeted to postsynaptic elements.

If the increased receptor abundance in ventral cord puncta were due to the inability to ubiquitinate the mutant receptors, then we would predict that mutant receptors lacking these cytosolic lysine residues would not form Ub-GLR-1 conjugates. We directly tested this possibility in double immunoprecipitation experiments. We found that GLR-1(4KR) mutant receptors formed significantly less Ub-GLR-1 conjugates than did the wild-type receptors (Figure 6C). Taken together, these results suggest that preventing ubiquitination of GLR-1::GFP caused increased accumulation of receptors at postsynaptic elements. However, it remains possible that mutating these lysine residues also has other effects on receptor function.

Our results thus far did not rule out the possibility that ubiquitination of other proteins, in addition to GLR-1, also contributes to ubiquitin-mediated regulation of GLR-1-containing synapses. To address this question, we coexpressed MUb and GLR-1(4KR) mutant receptors in transgenic animals. We found that GLR-1(4KR) puncta amplitudes were not diminished by MUb (Figure 7G). By contrast, expressing GLR-1(4KR) did not prevent the MUb-induced decrease in puncta density (Figures 7D, 7E, and 7I). These results suggest that formation of Ub-GLR-1 conjugates was necessary for ubiquitin-induced decreases in puncta amplitudes but that ubiquitination of other substrates may mediate the effects on the number or density of GLR-1-containing synapses.

Ubiquitination of GLR-1 and *unc-11* AP180 Act Together in a Single Process

Ubiquitin conjugation is involved in many intracellular processes—proteasomal degradation of cytosolic proteins or of misfolded and misassembled proteins in the endoplasmic reticulum, trafficking of membrane proteins in the golgi, endocytosis of plasma membrane proteins, and sorting of proteins from late endosomes to lysosomes (Hochstrasser, 1996; Hicke, 1999; Helliwell et al., 2001; Katzmann et al., 2001; Reggiori and Pelham, 2001; Urbanowski and Piper, 2001). Any of these effects could contribute to the ubiquitin-mediated regulation of GLR-1::GFP fluorescence. If ubiquitination were required for endocytosis of GLR-1 receptors, then ubiquitination of GLR-1 and *unc-11* AP180 should appear to act in a linear pathway. If ubiquitin were involved in any other aspect of GLR-1 assembly or targeting, then ubiquitination of GLR-1 and *unc-11* AP180 would be predicted to act as independent or parallel processes. We did several experiments to distinguish between these possibilities.

First, if ubiquitination of GLR-1 is required for receptor endocytosis, then ubiquitin-induced degradation of GLR-1::GFP should be prevented by blocking endocytosis. Consistent with this prediction, we found that *unc-11* AP180 puncta amplitudes were not significantly decreased by MUb and the effect on puncta densities was greatly reduced (Figures 3C and 3D).

Second, if ubiquitination and *unc-11* AP180 act in independent or parallel processes, both of which decrease the levels of GLR-1::GFP in ventral cord puncta, then one would predict that the defects caused by *unc-11* AP180 and by GLR-1(4KR) mutations would be additive, i.e., the defects observed in the *unc-11* AP180; *nuIs108* GLR-1(4KR)::GFP double mutants would be more severe than either single mutant. In fact, we found that the puncta width distributions for *unc-11* AP180 and for *unc-11* AP180; *nuIs108* GLR-1(4KR)::GFP were indistinguishable (Figures 7H and 7J).

Third, if Ub-GLR-1 conjugates were removed from the ventral cord by endocytosis, then blocking endocytosis should cause Ub-GLR-1 conjugates to accumulate. Consistent with this idea, we found that Ub-GLR-1::GFP conjugates were 2-fold more abundant in *unc-11* AP180 mutants than in wild-type controls (Figures 6D and 6E). These results suggest that *unc-11* AP180 mediates the degradation of Ub-GLR-1 conjugates.

Taken together, these results are most consistent with the model that ubiquitination of GLR-1::GFP and *unc-11* AP180 act together in a single process. Therefore, we propose that ubiquitin conjugation triggers the removal of GLR-1::GFP from the postsynaptic plasma membrane, a process that is mediated by *unc-11* AP180 and clathrin-mediated endocytosis.

Ubiquitination of GLR-1 Regulates Locomotion Behavior

Thus far our results suggest that ubiquitination regulates the abundance of GLR-1 receptors at ventral cord puncta, and the number of puncta. If ubiquitin regulates the number of GLR-1 receptors in the postsynaptic plasma membrane, then it should regulate the strength of synaptic inputs. Consequently, we would expect ubiquitination of GLR-1 to regulate behaviors mediated by these synapses. *C. elegans* locomotion consists of an alternating pattern of forward and reverse sinusoidal movements. The GLR-1-expressing interneurons have been shown to play a critical role in locomotion (Chalfie et al., 1985; Wicks and Rankin, 1995; Zheng et al., 1999). GLR-1 receptors are expressed in interneurons required for forward (AVB and PVC) and backward (AVA and AVD) locomotion (Figure 8A). Glutamatergic input to these interneurons, provided by several classes of sensory neurons (White et al., 1986), has been shown to bias the locomotion circuit toward producing backward movement (Zheng et al., 1999). This effect is illustrated by the prolonged duration of forward locomotion in *eat-4* VGLUT mutants (Figure 8B), which are defective for synaptic release of glutamate (Lee et al., 1999; Bellochio et al., 2000; Takamori et al., 2000), as previously reported (Zheng et al., 1999). Conversely, expressing mutant GLR-1 receptors that are constitutively open caused a dramatic decrease in the duration of forward movements (Zheng et al., 1999). Similarly, we found that *nuIs108* GLR-1(4KR)::GFP mutants had significantly shorter periods of forward locomotion than were observed in *nuIs24* GLR-1::GFP animals (Figure 8B), as would be expected if synaptic inputs had been strengthened. The difference in the locomotion behavior of these two strains cannot be ascribed to a difference in GLR-1 expression levels since *nuIs108* GLR-1(4KR)::GFP animals expressed less total GLR-1 receptor than did *nuIs24* GLR-1::GFP animals (Table 1). However, the behavioral defect observed in *nuIs108* GLR-1(4KR)::GFP mutants could be caused by nonsynaptic receptors rather than by a change in synaptic transmission. To address this possibility, we analyzed the behavior of *eat-4* VGLUT; *nuIs108* GLR-1(4KR)::GFP double mutants. We found that preventing synaptic release of glutamate (with the *eat-4* VGLUT mutation) blocked the effect of *nuIs108* GLR-1(4KR)::GFP on the duration of forward locomotion (Figure 8B). These results show that the effects of *nuIs108* GLR-1(4KR)::GFP on locomotion are mediated by synaptic GLR-1 receptors. Although we are unable to measure synaptic strength directly, these behavioral data suggest that preventing ubiquitination of GLR-1 resulted in increased synaptic strength.

Discussion

Recent work in a variety of systems suggests that an important mechanism for regulating synaptic strength

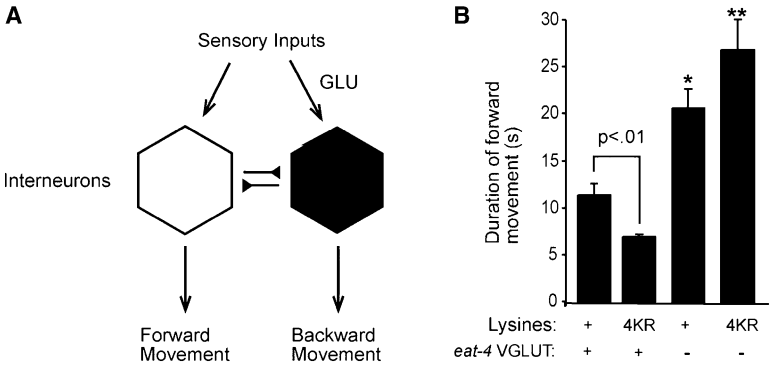

Figure 8. Lysine Mutations Alter Locomotion Behavior

(A) A simplified version of the neural circuit for locomotion is illustrated. GLR-1-expressing interneurons drive either forward (AVB and PVC, white hexagons) or backward (AVA and AVD, black hexagons) sinusoidal movements. The forward and backward interneurons form extensive reciprocal synaptic connections (White et al., 1986). Glutamatergic inputs (provided by sensory neurons) bias the circuit toward producing backward movement, as previously shown (Zheng et al., 1999). (B) The duration of forward locomotion movements are compared for wild-type (*nuls24* GLR-1::GFP), 4KR [*nuls108* GLR-1(4KR)::GFP], *eat-4* (*eat-4; nuls24* GLR-1::GFP), and *eat-4;* 4KR [*eat-4; nuls108* GLR-1(4KR)::GFP] double mutants. Values shown are mean ± standard errors. * This value significantly differs ($p < 0.001$) from the wild-type control. **This value differs significantly ($p < 0.0001$) from the 4KR single mutant.

is the regulation of the abundance of AMPA receptors at postsynaptic elements. Here we tested the role of ubiquitination in regulating the abundance of AMPA receptors at neuron-neuron synapses and the strength of these synapses. Our work leads to several conclusions. First, GLR-1::GFP is removed from postsynaptic elements by clathrin-mediated endocytosis, and this process requires the monomeric clathrin adaptin protein *unc-11* AP180. Second, a significant fraction of endocytosed *glr-1* GluRs is degraded. Third, ubiquitin controls two independent aspects of GLR-1-containing synapses: reducing both the amount of receptor at each postsynaptic element and reducing the density of postsynaptic elements in the ventral cord. Fourth, *glr-1* GluRs are directly modified by ubiquitination, and ubiquitination of GLR-1::GFP is largely responsible for ubiquitin-induced decreases in receptor abundance at synapses. Fifth, ubiquitination of GLR-1::GFP is unlikely to explain ubiquitin-induced decreases in the density of synapses, implying that ubiquitination of other proteins mediate this effect. Sixth, preventing ubiquitination of GLR-1 altered locomotion behavior in a manner consistent with an increase in synaptic strength. Taken together, our results suggest that ubiquitination of GLR-1 receptors plays an important role in regulating synaptic strength via regulating the abundance of receptors at the postsynaptic membrane, that ubiquitin also regulates formation or stability of GLR-1-containing synapses, and that AP180 is required for both of these processes.

Ubiquitination of GLR-1 Receptors

One potential caveat for our results is that the Ub-GLR-1 conjugates we observed are a consequence of overexpression of either ubiquitin or of chimeric GLR-1::GFP receptors. We provide several experiments that argue against this possibility. Ub-GLR-1 conjugates were formed both with transgene-encoded MUb, and with endogenously expressed ubiquitin. Thus, formation of Ub-GLR-1 conjugates was not caused by overexpression of ubiquitin. We were unable to detect Ub-GLR-1 conjugates formed with endogenously expressed receptors and ubiquitin; however, this is not surprising given the small fraction of total receptors (<1%) we expect to find in such complexes and the relative insensitivity of our anti-GLR-1 antisera. The ubiquitination motif we define in GLR-1 (Figure 5B) is conserved in mammalian AMPA receptors, and deletion of this motif in rat GluR2 was previously shown to increase receptor abundance in the plasma membrane of neurons (Lin et al., 2000). This conserved motif bears some similarity to ubiquitin-endocytosis signals found in yeast Ste2p and Ste6p. Conservation of this motif, and conservation of its function in regulating receptor abundance, suggest that ubiquitination is not a consequence of experimental overexpression of GLR-1 receptors. Therefore, although we were unable to directly document the formation of Ub-GLR-1 conjugates formed with endogenously expressed receptors, our results are most consistent with the hypothesis that ubiquitination of AMPA receptors is a conserved mechanism regulating their abundance at synapses.

Endocytic Trafficking of GLR-1 Receptors

Previous studies showed that an important mechanism for regulating synaptic strength is the removal of AMPA receptors from the postsynaptic membrane by clathrin-mediated endocytosis (Nishimune et al., 1998; Song et al., 1998; Carroll et al., 1999a, 1999b; Luscher et al., 1999; Luthi et al., 1999; Man et al., 2000; Wang and Linden, 2000). The mechanisms by which AMPA receptors are removed from synapses appear diverse. Removal can be triggered by treatment with NMDA, AMPA, metabotropic GluR agonists, AMPA receptor antagonists, and insulin. In each case, the signaling pathways required for receptor internalization and the fate of the internalized receptors appear to be distinct. Our work suggests that one mechanism by which receptors are removed from synapses is ubiquitination of conserved cytosolic lysine residues in AMPA receptors.

Our results demonstrate that mutants lacking the *unc-11* AP180 clathrin adaptin accumulate abnormally high levels of GLR-1::GFP in the ventral nerve cord and that this defect arises from absence of *unc-11* AP180 in the GLR-1-expressing interneurons. These results are complementary to those obtained with mammalian AMPA receptors. Several labs have shown that internalization of rat GluRs is mediated by clathrin, the clathrin adaptin AP2, and dynamin (Carroll et al., 1999a, 1999b; Luscher et al., 1999; Man et al., 2000). The post-endocytic fate of rat GluRs has been analyzed in a few cases (Ehlers,

2000; Lin et al., 2000; Liang and Huganir, 2001), where it was shown that receptors were either recycled back to the plasma membrane or targeted to lysosomes. Interestingly, different treatments biased AMPA receptors toward either recycling (NMDA treatment) or targeting to late endosomes/lysosomes (AMPA treatment). In our case, a significant fraction of endocytosed GLR-1 receptors was apparently degraded (perhaps in lysosomes), as GLR-1::GFP fluorescence was increased in *unc-11* AP180 mutants. In analogy to mammalian AMPA receptors, we expect that a significant fraction of endocytosed GLR-1 receptors are also recycled; however, our fluorescence measurements are unable to detect receptor recycling.

What is the fate of ubiquitinated *glr-1* GluRs? Several results suggest that Ub-GLR-1 conjugates are removed from synapses by an *unc-11* AP180-mediated process. Overexpression of a MUb transgene greatly decreased GLR-1::GFP puncta amplitudes in the ventral nerve cord. This ubiquitin-induced decrease in puncta amplitude was prevented by an *unc-11* AP180 mutation or by expressing a mutant form of GLR-1 lacking cytoplasmic lysine residues. The effects of *unc-11* AP180 and GLR-1(4KR) mutations on receptor abundance at synapses were not additive. Finally, mutants lacking *unc-11* AP180 had increased levels of Ub-GLR-1 conjugates, suggesting that these conjugates were normally degraded by a process requiring *unc-11* AP180. Taken together, these results are most consistent with the hypothesis that *unc-11* AP180 and GLR-1 ubiquitination act together in a common process. Therefore, we propose that ubiquitination of cytoplasmic lysine residues on AMPA receptors constitutes a signal to remove the conjugated receptors from postsynaptic elements, and subsequently for targeting them for degradation.

What specific aspect of GLR-1 trafficking is regulated by ubiquitin? Two models are consistent with our results. Ubiquitination of cytoplasmic lysine residues might trigger removal of the conjugated receptors from the plasma membrane by clathrin-mediated endocytosis. Alternatively, GLR-1 receptors delivered to endosomes, by either constitutive or stimulated endocytosis, are ubiquitinated in the limiting membrane of late endosomes, leading to their internalization into multivesicular bodies, and delivery to lysosomes. There are precedents for both of these mechanisms (Hicke, 1999; Katzmann et al., 2001; Reggiori and Pelham, 2001; Urbanowski and Piper, 2001). For several reasons, we favor the former hypothesis. First, the AP180 adaptin protein is required for removal of proteins from the plasma membrane by clathrin-mediated endocytosis in both *Drosophila* and *C. elegans* (Zhang et al., 1998; Nonet et al., 1999). Since our results indicate that ubiquitin acts prior to AP180, we infer that Ub-GLR-1 conjugates form in the plasma membrane. Second, the GLR-1 ubiquitination motif defined here shares some core sequences with ubiquitination/endocytosis signals in the yeast Ste2p and Ste6p proteins (Figure 6). Third, deletion of sequences corresponding to this ubiquitination motif produced defects in AMPA-induced endocytosis of rat GluR2 (Lin et al., 2000). Interestingly, both AMPA-induced endocytosis of GluR2 (Ehlers, 2000) and AP180-mediated endocytosis of GLR-1 lead to receptor degradation. Given the similarity of the GLR-1 ubiquitination motif (Figure 6) and the GluR2 endocytosis signal (Lin et al., 2000), we propose that ubiquitination of GLR-1 may be induced by glutamate binding. Fourth, expressing mutant GLR-1(4KR) receptors, which were not ubiquitinated, produced locomotion defects that were similar to those caused by mutations that constitutively activate GLR-1. Furthermore, this behavioral effect was dependent upon synaptically released glutamate. Thus, the effect of the GLR-1(4KR) mutation on locomotion strongly implies that synaptic strength is regulated by formation of Ub-GLR-1 conjugates. On the other hand, our results do not exclude the possibility that AP180 also plays a role in endosome-lysosome trafficking. In any of these scenarios, our results strongly support the idea that ubiquitination of GLR-1 receptors regulates their abundance at neuron-neuron synapses, and thereby alters synaptic strength.

Implications for Synapse Formation and Plasticity

Several studies have shown that activity regulates the abundance of AMPA receptors at central synapses, and that these changes occur over a broad range of time scales. Rapid delivery of AMPA receptors to dendritic spines is promoted by treatments or patterns of activity that promote long-term potentiation (Shi et al., 1999, 2001; Hayashi et al., 2000) whereas treatments that promote long-term depression promote removal of AMPA receptors by endocytosis (Carroll et al., 1999b). Over longer time scales, homeostatic mechanisms have been described whereby neurons globally scale up or down the abundance of AMPA receptors at all of their synapses (Craig, 1998; Turrigiano, 1999). Long-term activity blockade causes increased accumulation of AMPA receptors at postsynaptic elements whereas long-term enhancement of activity leads to decreased AMPA receptor abundance at postsynaptic elements in cultured neurons. Our work suggests that, in some cases, changes in activity (either Hebbian or homeostatic) might alter the abundance of AMPA receptors at synapses by triggering formation of AMPA receptor-ubiquitin conjugates.

Previous studies implicated ubiquitin in presynaptic processes regulating synaptic growth and function (Hegde et al., 1997; Chain et al., 1999; DiAntonio et al., 2001). We show here that ubiquitination of a postsynaptic protein (GLR-1) regulates synapse structure and function. We also found that overexpression of ubiquitin significantly reduced the density of ventral cord puncta, suggesting that ubiquitin plays a role in the stability or formation of synapses. The ubiquitin-induced decrease in puncta density was diminished by *unc-11* AP180 mutations, implying that clathrin-mediated endocytosis was also involved in this process. However, we found that mutating cytosolic lysine residues in GLR-1 did not block the effects of ubiquitin on puncta density. Therefore, we speculate that ubiquitination of other synaptic proteins (i.e., in addition to GLR-1) will mediate the effects on puncta density. These unidentified proteins are also likely to be postsynaptic proteins, as overexpression of MUb in the GLR-1-expressing cells was sufficient to elicit the change in puncta density. Thus, it is likely that ubiquitination of both pre- and postsynaptic proteins will play important roles in synapse formation and plasticity.

Experimental Procedures

Strains

Standard methods were used to culture the following alleles: *glr-1(n2461)*, *unc-11(nu428)*, *unc-11(e47)*, *unc-64(e246)*, *snb-1(md247)*, *eat-4(n2474)*, *nuIs24* GLR-1::GFP, *nuIs25* GLR-1::GFP, *nuIs108* GLR-1(4KR)::GFP, *nuIs88* GLR-1(K888R)::GFP, *nuIs89* MUb. Unless otherwise noted, all wild-type GLR-1::GFP results refer to *nuIs24*.

Isolation of *unc-11* AP180 Mutations

The *unc-11(nu428)* allele was isolated in a screen for mutants with altered GLR-1::GFP (*nuIs25*) fluorescence. *unc-11(e47)* was isolated previously as an uncoordinated mutant (Brenner, 1974). Both *e47* and *nu428* have a purely recessive pattern of heredity for the defects in GLR-1::GFP distribution.

Fluorescence Microscopy and Quantitative Analysis

All imaging experiments were done using a Zeiss Aviovert 100 microscope, and an ORCA CCD camera (Hamamatsu). Animals were immobilized with 10 mM levamisole. Images were captured and processed using Metamorph 4.5 software (Universal Imaging).

For quantitative studies of puncta fluorescence, we used an Olympus Planapo 100× (NA = 1.4) objective. Maximum intensity projections of Z series stacks were obtained. Identical camera gain, exposure settings, and fluorescence filters were used for all images and results reported. Using these conditions, GFP fluorescence filled the 12-bit dynamic range, without saturation. Line scans of ventral cord fluorescence were analyzed in Igor Pro (WaveMetrics) using custom-written software.

Each line scan corresponds to approximately 80 μm of the ventral cord. All images were taken in a single region of the ventral cord (lying between the RIG neurons and the vulva). Puncta dimensions, intensities, and densities were estimated in an automated manner in Igor. To control for changes in illumination intensity, values were normalized with respect to background fluorescence on each slide.

Puncta amplitudes were calculated as the fractional increase in peak fluorescence over the diffuse background of fluorescence in the ventral cord (ΔF/F). Puncta widths were estimated as the peak width at half-maximal amplitudes. Puncta densities were measured as the average number of puncta in 10 μm of ventral cord length. All values reported in figures are means ± standard errors. Statistical significance was determined by two-tailed Student's t test. The number of line scans and puncta analyzed for each genotype are reported in Table 1.

The extent of colocalization of GLR-1 with presynaptic markers (synaptobrevin or *eat-4* VGLUT) was determined in an automated manner. CFP- and YFP-tagged proteins coexpressed in transgenic animals were simultaneously imaged. Fluorescent filter sets (Chroma) were as follows: excitation (D436/10X, HQ500/20X), emission (D470/30M, HQ535/30M), cyan/topaz polychroic mirror. Maximum intensity projections of the CFP and YFP images were overlayed. The spatial position of the CFP and YFP peaks was recorded as the position of the local maximum in each punctum. The fraction of GLR-1 puncta that were colocalized with a presynaptic punctum was determined by the percentage of GLR-1 puncta that had peaks that were less than 1 μm (or the width of an average punctum) from a presynaptic peak.

Transgenes and Germline Transformation

Plasmids were constructed by standard techniques; full details are available on request. Transgenic strains were isolated by microinjecting various plasmids (typically at 10–100 ng/μl) using either *ttx-3::gfp* (O. Hobert) or GLR-1::GFP as a marker. Stable integrated transgenes were obtained from extrachromosomal arrays after UV irradiation. Point mutations were introduced into plasmids using the Quickchange mutagenesis kit (Stratagene). The *nuIs108* GLR-1(4KR)::GFP transgene contains KP#647, which encodes GLR-1::GFP with the K888R, K900R, K903R, and K944R mutations. The *nuIs88* GLR-1(K888R)::GFP transgene contains KP#726, which encodes GLR-1::GFP with the K888R mutation. The KP#565 and KP#587 plasmids encode GLR-1::YFP and GLR-1::CFP, respectively. The KP#674 and KP#826 plasmids encode GLR-1(4KR)::YFP and GLR-1(4KR)::CFP, respectively. The plasmids KP#215 and KP#228 contain the CFP::SNB-1 fusion gene expressed with the *glr-1* promoter and the *mec-3* promoters, respectively. CFP was fused at the predicted amino terminus of SNB-1. The plasmid KP#748 contains a 5.9 kb *eat-4* promoter driving the expression of a YFP-tagged EAT-4 protein. The transgene *nuIs89* MUb contains the plasmid KP#727 which encodes nine copies of the Myc epitope fused to the amino terminus of yeast ubiquitin (M. Hochstrasser) expressed by the *glr-1* promoter. The plasmid KP#532 encodes MUb(K48R), expressed by the *glr-1* promoter. KP#546, 547, 548, and 549 contain wild-type *unc-11* AP180 cDNAs (types A–E, respectively), expressed by the *glr-1* promoter (Nonet et al., 1999). For rescue of the *unc-11* phenotype, the plasmids KP#546, 547, 548, 550, and 549 were pooled together and coinjected into *unc-11(e47); nuIs24* GLR-1::GFP animals.

Antisera, Immunoprecipitations, and Western Blots

Rabbit anti-GFP antibodies were made as described (Seedorf et al., 1999). Antibodies were obtained as follows: monoclonal anti-GFP Roche (Indianapolis, Indiana), monoclonal anti-ubiquitin Covance (Princeton, New Jersey), rabbit anti-ubiquitin (C. Shamu and T. Rapoport) (Shamu et al., 1999), and peroxidase-coupled anti-mouse Amersham. Extracts were prepared from mixed stage worms with a French Press in buffer A (50 mM Hepes [pH 7.7], 50 mM potassium acetate, 2 mM magnesium acetate, 1 mM EDTA, 250 mM sucrose), protease inhibitors (10 μg/ml leupeptin, 5 μg/ml chymostatin, 3 μg/ml elastatinal, 1 μg/ml pepstatin A, 1 mM PMSF), and 10 mM N-ethylmaleimide. Membranes were isolated from the clarified extract by spinning at 300,000 × g. Membranes were resuspended in buffer A plus 7 mM β-mercaptoethanol, solubilized with 1 volume SDS buffer (50 mM Tris-HCl [pH 8.5], 1% SDS, 2 mM DTT), then diluted with 5 volumes 50 mM Hepes (pH 7.7), 600 mM NaCl, 1% NP-40. Immunoprecipitates were formed with anti-GFP serum and a mixture of protein A- and G-sepharose beads (Pharmacia). All immunoprecipitations reported were repeated on at least three independent membrane preps for each genotype. GLR-1::GFP was detected with anti-GFP using enhanced chemiluminescence (Pierce). Abundance of GLR-1::GFP in different transgenic strains was expressed as a fraction of the total protein concentrations in worm extracts (Table 1). Protein concentrations were determined using BCA reagent (Pierce).

Analysis of Locomotion Behavior

The duration of forward and reverse locomotion movements of day one adult hermaphrodites was determined as previously described (Zheng et al., 1999). Briefly, individual adult worms were observed for 5 min and a computer program keyed by the observer recorded the duration of forward and reverse movements. Locomotion assays were done by an experimenter unaware of the genotype of the animals being analyzed.

Acknowledgments

The authors thank the following for strains, plasmids, antisera, and advice: C. Shamu, T. Rapoport, M. Nonet, A. Fire, M. Hochstrasser, P. Silver, S. Emr, D. Gregorio, and G. Garriga. We thank the members of the Kaplan lab for comments on the manuscript. This work was supported by a grant from the NIH to J.K. (NS32196). L.D. was supported by a postdoctoral fellowship from the NIH (F32 NS41705). J.D. was supported by a postdoctoral fellowship from the Damon Runyon Walter Winchell Foundation (DRG 1623). M.G. was supported by a postdoctoral fellowship (0020046Y) from the American Heart Association, California Division.

Received: November 2, 2001
Revised: April 30, 2002

References

Beattie, E.C., Carroll, R.C., Yu, X., Morishita, W., Yasuda, H., von Zastrow, M., and Malenka, R.C. (2000). Regulation of AMPA receptor endocytosis by a signaling mechanism shared with LTD. Nat. Neurosci. *3*, 1291–1300.

Bellochio, E., Reimer, R., Fremeau, R., and Edwards, R. (2000). Up-

take of glutamate into synaptic vesicles by an inorganic phosphate transporter. Science *289*, 957–960.

Brenner, S. (1974). The genetics of Caenorhabditis elegans. Genetics *77*, 71–94.

Brockie, P.J., Madsen, D.M., Zheng, Y., Mellem, J., and Maricq, A.V. (2001). Differential expression of glutamate receptor subunits in the nervous system of Caenorhabditis elegans and their regulation by the homeodomain protein UNC-42. J. Neurosci. *21*, 1510–1522.

Carroll, R.C., Beattie, E.C., Xia, H., Luscher, C., Altschuler, Y., Nicoll, R.A., Malenka, R.C., and von Zastrow, M. (1999a). Dynamin-dependent endocytosis of ionotropic glutamate receptors. Proc. Natl. Acad. Sci. USA *96*, 14112–14117.

Carroll, R.C., Lissin, D.V., von Zastrow, M., Nicoll, R.A., and Malenka, R.C. (1999b). Rapid redistribution of glutamate receptors contributes to long-term depression in hippocampal cultures. Nat. Neurosci. *2*, 454–460.

Chain, D.G., Casadio, A., Schacher, S., Hegde, A.N., Valbrun, M., Yamamoto, N., Goldberg, A.L., Bartsch, D., Kandel, E.R., and Schwartz, J.H. (1999). Mechanisms for generating the autonomous cAMP-dependent protein kinase required for long-term facilitation in Aplysia. Neuron *22*, 147–156.

Chalfie, M., Sulston, J.E., White, J.G., Southgate, E., Thomson, J.N., and Brenner, S. (1985). The neural circuit for touch sensitivity in C. elegans. J. Neurosci. *5*, 956–964.

Craig, A.M. (1998). Activity and synaptic receptor targeting: the long view. Neuron *21*, 459–462.

DiAntonio, A., Haghighi, A.P., Portman, S.L., Lee, J.D., Amaranto, A.M., and Goodman, C.S. (2001). Ubiquitination-dependent mechanisms regulate synaptic growth and function. Nature *412*, 449–452.

Ehlers, M.D. (2000). Reinsertion or degradation of AMPA receptors determined by activity-dependent endocytic sorting. Neuron *28*, 511–525.

Hart, A., Sims, S., and Kaplan, J. (1995). A synaptic code for sensory modalities revealed by analysis of the C. elegans GLR-1 glutamate receptor. Nature *378*, 82–85.

Hayashi, Y., Shi, S.H., Esteban, J.A., Piccini, A., Poncer, J.C., and Malinow, R. (2000). Driving AMPA receptors into synapses by LTP and CaMKII: requirement for GluR1 and PDZ domain interaction. Science *287*, 2262–2267.

Hegde, A.N., Inokuchi, K., Pei, W., Casadio, A., Ghirardi, M., Chain, D.G., Martin, K.C., Kandel, E.R., and Schwartz, J.H. (1997). Ubiquitin C-terminal hydrolase is an immediate-early gene essential for long-term facilitation in Aplysia. Cell *89*, 115–126.

Helliwell, S.B., Losko, S., and Kaiser, C.A. (2001). Components of a ubiquitin ligase complex specify polyubiquitination and intracellular trafficking of the general amino acid permease. J. Cell Biol. *153*, 649–662.

Hicke, L. (1999). Gettin' down with ubiquitin: turning off cell-surface receptors, transporters and channels. Trends Cell Biol. *9*, 107–112.

Hochstrasser, M. (1996). Ubiquitin-dependent protein degradation. Annu. Rev. Genet. *30*, 405–439.

Jiang, Y.H., Armstrong, D., Albrecht, U., Atkins, C.M., Noebels, J.L., Eichele, G., Sweatt, J.D., and Beaudet, A.L. (1998). Mutation of the Angelman ubiquitin ligase in mice causes increased cytoplasmic p53 and deficits of contextual learning and long-term potentiation. Neuron *21*, 799–811.

Katzmann, D., Babst, M., and Emr, S. (2001). Ubiquitin-dependent sorting into the multivesicular body pathway requires function of a conserved endosomal protein sorting complex, ESCRT-1. Cell *106*, 145–155.

Kirchhausen, T. (1999). Adaptors for clathrin-mediated traffic. Annu. Rev. Cell Dev. Biol. *15*, 705–732.

Lee, R.Y.N., Sawin, E.R., Chalfie, M., Horvitz, H.R., and Avery, L. (1999). EAT-4, a homolog of a mammalian sodium-dependent inorganic phosphate cotransporter, is necessary for glutamatergic neurotransmission in caenorhabditis elegans. J. Neurosci. *19*, 159–167.

Liang, F., and Huganir, R.L. (2001). Coupling of agonist-induced AMPA receptor internalization with receptor recycling. J. Neurochem. *77*, 1626–1631.

Lin, J.W., Ju, W., Foster, K., Lee, S.H., Ahmadian, G., Wyszynski, M., Wang, Y.T., and Sheng, M. (2000). Distinct molecular mechanisms and divergent endocytotic pathways of AMPA receptor internalization. Nat. Neurosci. *3*, 1282–1290.

Lledo, P.M., Zhang, X., Sudhof, T.C., Malenka, R.C., and Nicoll, R.A. (1998). Postsynaptic membrane fusion and long-term potentiation. Science *279*, 399–403.

Lu, W., Man, H., Ju, W., Trimble, W.S., MacDonald, J.F., and Wang, Y.T. (2001). Activation of synaptic NMDA receptors induces membrane insertion of new AMPA receptors and LTP in cultured hippocampal neurons. Neuron *29*, 243–254.

Luscher, C., Xia, H., Beattie, E.C., Carroll, R.C., von Zastrow, M., Malenka, R.C., and Nicoll, R.A. (1999). Role of AMPA receptor cycling in synaptic transmission and plasticity. Neuron *24*, 649–658.

Luthi, A., Chittajallu, R., Duprat, F., Palmer, M.J., Benke, T.A., Kidd, F.L., Henley, J.M., Isaac, J.T., and Collingridge, G.L. (1999). Hippocampal LTD expression involves a pool of AMPARs regulated by the NSF-GluR2 interaction. Neuron *24*, 389–399.

Man, H.Y., Lin, J.W., Ju, W.H., Ahmadian, G., Liu, L., Becker, L.E., Sheng, M., and Wang, Y.T. (2000). Regulation of AMPA receptor-mediated synaptic transmission by clathrin-dependent receptor internalization. Neuron *25*, 649–662.

Maricq, A.V., Peckol, E., Driscoll, M., and Bargmann, C. (1995). glr-1, a C. elegans glutamate receptor that mediates mechanosensory signaling. Nature *378*, 78–81.

Nishimune, A., Isaac, J.T., Molnar, E., Noel, J., Nash, S.R., Tagaya, M., Collingridge, G.L., Nakanishi, S., and Henley, J.M. (1998). NSF binding to GluR2 regulates synaptic transmission. Neuron *21*, 87–97.

Nonet, M.L., Holgado, A.M., Brewer, F., Serpe, C.J., Norbeck, B.A., Holleran, J., Wei, L., Hartwieg, E., Jorgensen, E.M., and Alfonso, A. (1999). UNC-11, a Caenorhabditis elegans AP180 homologue, regulates the size and protein composition of synaptic vesicles. Mol. Biol. Cell *10*, 2343–2360.

Papa, F.R., and Hochstrasser, M. (1993). The yeast DOA4 gene encodes a deubiquitinating enzyme related to a product of the human tre-2 oncogene. Nature *366*, 313–319.

Passafaro, M., Piech, V., and Sheng, M. (2001). Subunit-specific temporal and spatial patterns of AMPA receptor exocytosis in hippocampal neurons. Nat. Neurosci. *4*, 917–926.

Reggiori, F., and Pelham, H.R. (2001). Sorting of proteins into multivesicular bodies: ubiquitin-dependent and -independent targeting. EMBO J. *20*, 5176–5186.

Rongo, C., and Kaplan, J. (1999). CaMKII regulates the density of central glutamatergic synapses in vivo. Nature *402*, 195–199.

Rongo, C., Whitfield, C.W., Rodal, A., Kim, S.K., and Kaplan, J.M. (1998). LIN-10 is a shared component of the polarized protein localization pathways in neurons and epithelia. Cell *94*, 751–759.

Seedorf, M., Damelin, M., Kahana, J., Taura, T., and Silver, P.A. (1999). Interactions between a nuclear transporter and a subset of nuclear pore complex proteins depend on Ran GTPase. Mol. Cell. Biol. *19*, 1547–1557.

Shamu, C.E., Story, C.M., Rapoport, T.A., and Ploegh, H.L. (1999). The pathway of US11-dependent degradation of MHC class I heavy chains involves a ubiquitin-conjugated intermediate. J. Cell Biol. *147*, 45–58.

Shi, S., Hayashi, Y., Esteban, J.A., and Malinow, R. (2001). Subunit-specific rules governing ampa receptor trafficking to synapses in hippocampal pyramidal neurons. Cell *105*, 331–343.

Shi, S.H., Hayashi, Y., Petralia, R.S., Zaman, S.H., Wenthold, R.J., Svoboda, K., and Malinow, R. (1999). Rapid spine delivery and redistribution of AMPA receptors after synaptic NMDA receptor activation. Science *284*, 1811–1816.

Snyder, E.M., Philpot, B.D., Huber, K.M., Dong, X., Fallon, J.R., and Bear, M.F. (2001). Internalization of ionotropic glutamate receptors in response to mGluR activation. Nat. Neurosci. *4*, 1079–1085.

Song, I., Kamboj, S., Xia, J., Dong, H., Liao, D., and Huganir, R.L. (1998). Interaction of the N-ethylmaleimide-sensitive factor with AMPA receptors. Neuron *21*, 393–400.

Swaminathan, S., Amerik, A.Y., and Hochstrasser, M. (1999). The

Doa4 deubiquitinating enzyme is required for ubiquitin homeostasis in yeast. Mol. Biol. Cell *10*, 2583–2594.

Takamori, S., Rhee, J.S., Rosenmund, C., and Jahn, R. (2000). Identification of a vesicular glutamate transporter that defines a glutamatergic phenotype in neurons. Nature *407*, 189–194.

Thrower, J.S., Hoffman, L., Rechsteiner, M., and Pickart, C.M. (2000). Recognition of the polyubiquitin proteolytic signal. EMBO J. *19*, 94–102.

Turrigiano, G.G. (1999). Homeostatic plasticity in neuronal networks: the more things change, the more they stay the same. Trends Neurosci. *22*, 221–227.

Urbanowski, J.L., and Piper, R.C. (2001). Ubiquitin sorts proteins into the intralumenal degradative compartment of the late-endosome/vacuole. Traffic *2*, 622–630.

Wang, Y.T., and Linden, D.J. (2000). Expression of cerebellar long-term depression requires postsynaptic clathrin-mediated endocytosis. Neuron *25*, 635–647.

White, J.G., Southgate, E., Thomson, J.N., and Brenner, S. (1986). The structure of the nervous system of Caenorhabditis elegans. Philos. Trans. R Soc. Lond. *314*, 1–340.

Wicks, S.R., and Rankin, C.H. (1995). Integration of mechanosensory stimuli in C. elegans. J. Neurosci. *15*, 2434–2444.

Zhang, B., Koh, Y.H., Beckstead, R.B., Budnik, V., Ganetzky, B., and Bellen, H.J. (1998). Synaptic vesicle size and number are regulated by a clathrin adaptor protein required for endocytosis. Neuron *21*, 1465–1475.

Zheng, Y., Brockie, P.J., Mellem, J.E., Madsen, D.M., and Maricq, A.V. (1999). Neuronal control of locomotion in C. elegans is modified by a dominant mutation in the GLR-1 ionotropic glutamate receptor. Neuron *24*, 347–361.